

The long-term optical behavior of BL Lac object S5 0716+714

ZHANG BingKai^{1*}, DAI BenZhong², ZHANG Li² & CAO Zhen³

¹Department of Physics, Fuyang Normal College, Fuyang 236041, China;

²Department of Physics, Yunnan University, Kunming 650091, China;

³Key Laboratory of Particle and Astrophysics, Institute of High Energy Physics, CAS, Beijing 100049, China

Received November 2, 2009; accepted November 12, 2009

BL Lac object S5 0716+714 is a well-studied object. In this paper, the available optical (*BVRI*) data of this source are compiled, and the *B*-, *V*-, *R*- and *I*-band light curves are constructed. Each of them is analyzed by means of the discrete correlation function (DCF) method, the structure function (SF) method and the *z*-transformed discrete correlation function (ZDCF) method. The results imply that there is a possible periodic variation of 1211 days in each passband light curve. The source varies violently and complicatedly, and exhibits a brightening trend in the light curves.

BL Lacertae objects, S5 0716+714, optical behavior

PACS: 98.54.Cm, 95.85.Kr, 95.75.Wx

1 Introduction

As a special subclass of active galactic nuclei (AGNs), blazars include BL Lacertae objects and flat-spectrum radio quasars. They are widely studied at all wavelengths in recent years. They show some extreme properties: rapid and large variability, high and variable polarization, and no or only weak emission lines. But the nature of AGNs is still an open question. Variability analysis is one of the most important tools in studying the nature of AGNs, because much valuable information on the physics of AGNs lies in the amplitude of variation [1]. From observations of blazars, it is known that they vary on diverse time scales ranging from a few minutes to several years. Blazar variability can be broadly divided into three classes viz. intra-day variability (IDV) or intra-night variability or micro-variability, short term variability and long term variability. Periodicity analysis is an important part of the variability studies because the stable periodicities can help us locate the relevant physical parameters in AGNs. Some particular objects are claimed to display periodicity in their light curves over a variety of timescales [1–9].

The radio source S5 0716+714 was discovered in 1979 [10], and was classified as a BL Lac object because of its fea-

tureless spectrum and its strong optical polarization [11]. By optical imaging of the underlying galaxy, its redshift of $z = 0.31 \pm 0.08$ was derived recently by Nilsson et al. [12]. The source is a highly variable object and exhibits strong variability both on timescales of months [13] and on timescales of days and hours [14–20]. Quasi-periodic oscillations of S5 0716+714 have also been studied. Early in 1990 February, the light curves showed a change in the typical variability timescale from 1 day to 7 days [18,21]. Sagar et al. found that events with large amplitude ($\geq 1\text{mag}$) had almost the same duration of about 30 days [22]. Katajainen et al. found that the maximum point in its light curve would seem to occur with a period of 60–70 days [23]. Qian et al. also found evidence of quasi-periodic oscillations in their observations, and there may be a period on the order of 10 days in its light curve [24]. Ma et al. obtained one possible medium-timescale variation with a period of around 14 days [25]. Raiteri et al. found there may be an oscillation on a 3.3 year time scale in the *R* band light curve [26].

Our goal in this paper is to search for the possible long-term variable period in the historical optical light curves of BL Lac object S5 0716+714. Due to unevenly sampled monitoring data, the discrete correlation function (DCF) method and the structure function (SF) method as well as *z*-transformed discrete correlation function (ZDCF) method are employed.

*Corresponding author (email: zhangbk@mail.ihep.ac.cn)

2 The historical optical light curves

The source S5 0716+714 has been studied intensively and some light curves have been published. All available optical *BVRI*-band data on this source are compiled. These data are from the literature [13,20,23,24,26–28]. In sum, 23307 data points are collected. In order to estimate the total variability of each light curve, the fractional variability amplitude F_{var} is calculated, which is known as

$$F_{\text{var}} = \sqrt{\frac{S^2 - \bar{\varepsilon}_{\text{err}}^2}{\bar{x}^2}}, \quad (1)$$

where S^2 is the sample variance of the light curve, \bar{x} is the average flux and $\bar{\varepsilon}^2$ is the mean of the squared measurement uncertainties [29,30]. The detailed statistics and variabilities of these data are listed in Table 1. The first column represents the bands, the second represents the numbers, the third represents the mean values, the fourth represents the standard deviations, the fifth represents the largest variations and the last represents the fractional variability amplitudes. The full light curves of different passbands are displayed in Figure 1. They are very similar, and span more than 12 years.

From Figure 1, one can see a slight brightening trend in the historical light curves. On average, the source is brightening with amplitudes of 0.09, 0.07, 0.08 and 0.06 mag per year in the *B*, *V*, *R* and *I* passbands, respectively. In the optical *B*-band light curve, the long term brightening trend with a mean variation rate of 0.11 mag yr⁻¹ was also found by Nesci et al. [31].

Table 1 Statistics of *BVRI*-band data of BL Lac object S5 0716+714

Band	<i>N</i>	Mean (mag.)	σ (mag.)	Δ (mag.)	F_{var}
<i>B</i>	3499	13.83	0.60	3.11	0.043
<i>V</i>	4954	13.64	0.68	3.18	0.050
<i>R</i>	12701	13.23	0.50	2.90	0.038
<i>I</i>	2153	12.94	0.44	2.54	0.034

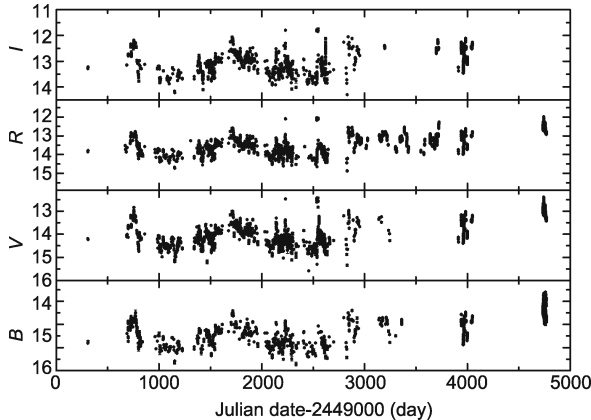


Figure 1 The full historical light curves of BL Lac object S5 0716+714. Most of the error bars are very small and invisible in the plots.

3 Period analysis methods

In general, there are several methods that can be used to search for periodicities [1]. In this work, three statistic methods are used: DCF, SF and ZDCF methods, which are the ideal methods for the unevenly sampled variability data. In this way, the results of the analysis can be cross-checked and be better confirmed.

3.1 The discrete correlation function method

The discrete correlation function (DCF) was introduced by some authors [32,33]. It can not only provide the correlation of two series of unevenly sampled variability data with the time lag, but also can give evidence of periods that lie in a single temporal data set. This method does not require interpolating in the temporal domain. Its other advantages are that it uses all the data points available and calculates a meaningful error estimate. The first step is to calculate the set of un-binned discrete correlations (UDCF) between each data point in the two data streams. It is defined as follows:

$$\text{UDCF}_{ij} = \frac{(a_i - \bar{a}) \times (b_j - \bar{b})}{\sqrt{\sigma_a^2 \times \sigma_b^2}}, \quad (2)$$

where a_i and b_j are points of the data sets a and b , \bar{a} and \bar{b} are the means of the data sets a and b , σ_a and σ_b are the standard deviations of each data set. Each of UDCF_{ij} is associated with the pair lag $\Delta t_{ij} = t_j - t_i$. Then we average over the M pairs for which $\tau - \Delta\tau/2 \leq \Delta t_{ij} < \tau + \Delta\tau/2$, and obtain DCF:

$$\text{DCF}(\tau) = \frac{1}{M} \sum \text{UDCF}_{ij}(\tau), \quad (3)$$

where M is the number of pairs in the bin. The standard error for each bin is defined as

$$\sigma(\tau) = \frac{1}{M-1} \{ \sum [\text{UDCF}_{ij} - \text{DCF}(\tau)]^2 \}^{1/2}. \quad (4)$$

When $a=b$, the autocorrelation DCF is produced, and when $a \neq b$, the cross-correlation DCF is measured. In most cases, the evident peak in the cross-correlation function means a strong correlation between two data series. The higher the peak, the stronger the correlation. The peak with a value equaling one in the autocorrelation DCF implies a strong period in the data set. The choice of the bin size $\Delta\tau$ is governed by a trade-off between the desired accuracy in the mean calculation and the desired resolution in the description of the correlation curve. In practice, the results depend only weakly on the specific bin size chosen. In order to obtain statistically meaningful values for the time lags and the uncertainties, one must perform Monte Carlo simulations [26,34].

Z-transformed discrete correlation function (ZDCF) method is related to the discrete correlation function (DCF) [35]. It is a binning type of method and can be considered as an improvement of the DCF technique. And it is more robust than DCF method when applied to very sparsely and irregularly sampled light curves [36,37]. The ZDCF differs in a

number of ways from the DCF, a notable feature being that the data are binned by equal population rather than into time bins of equal width $\Delta\tau$. One advantage of this technique is that it allows direct estimation of the uncertainties on the lag without the use of more assumption-dependent Monte Carlo simulations.

3.2 The structure function method

The structure function (SF) can potentially provide information on the nature of the physical process causing any observed variability. This method has several significant advantages. It is much easier to calculate and less affected by gaps in the light curves [38]. The definitions of SFs and their properties are presented in some literature [39–42]. The first-order SF is defined as

$$SF(\tau) = \frac{1}{N} \sum [a(t) - a(t + \tau)]^2, \quad (5)$$

where $a(t)$ is a point of the time series $\{a\}$, and the summation is made over all pairs separated in time by Δt which belongs to the interval $[\tau - \Delta\tau/2, \tau + \Delta\tau/2]$. The $\Delta\tau$ is a free parameter similar to that in the case of the DCF. The term N is the number of such pairs. If a periodic signal with time scale of P does exist in the light curve, the SF will show minima at $\tau = P$, with a value approaching zero. When τ is extended to multiples of P , SF itself goes through a series of cycles [1,26,43–45].

4 Results

The autocorrelation DCF and SF are calculated with a bin size of 15 days to determine the period in the B passband light curve. To constrain the spurious effects, the original fluxes are averaged over 5 days. The DCF and SF results are plotted in the top and middle panel of Figure 2, respectively. In the top panel of Figure 2, one can obviously see the highest peak corresponding to 1200 days. The value of DCF is 0.5 ± 0.12 . To obtain a more reliable estimate of the position of the peak, the centroid of the DCF is calculated, which is the weighted average of all DCF points greater than 80% of DCF_{max} . The centroid is 1185 days. In the middle panel of Figure 2, the SFs show a minimum at the position of 1230 days. The results calculated by means of two methods are in good agreement with each other. As a separate check, the z -transformed discrete function (ZDCF) is calculated and plotted in the bottom panel of Figure 2. At the position of 1241 days, there is a ZDCF peak with the value of 0.41. Corresponding to this peak, the centroid is 1206 days. This means that 1185–1230 days is a possible period in the B passband light curve of S5 0716+714.

The bin size of $\Delta\tau$ may affect the results of DCF and SF slightly. So, the different bin sizes of 10 days and 20 days are also used in this analysis. The shapes of DCF and SF show no evidence of change, and the positions of DCF maximum and SF minimum also show no obvious shift. The results are

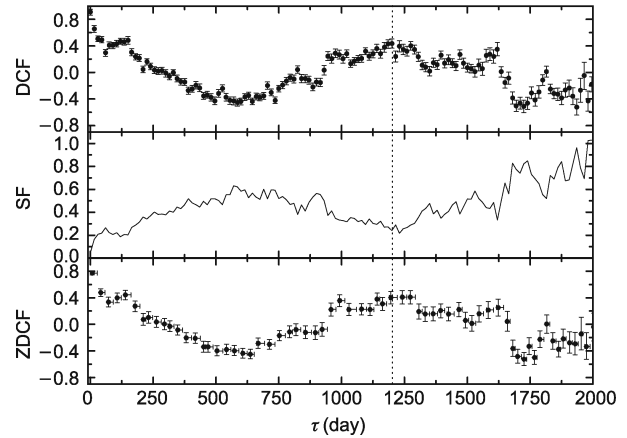


Figure 2 The DCF (top), SF (middle) and ZDCF (bottom) for the B passband. The vertical dotted line indicates the possible period according to the peak of DCF.

listed in Table 2. The first column is passbands, the second is the bin sizes, the third is the possible periods determined by the DCF method, the fourth is the possible period determined by the centroids corresponding to the DCF peaks, the fifth is the DCF values, the sixth is the possible periods obtained by the SF method, the seventh is the SF values, the eighth is the possible periods suggested by the ZDCF method, the ninth is the possible periods according to the centroids of the ZDCF peaks and the last column is the ZDCF peak values.

A similar analysis is also made in the V , R and I passband light curves. The DCFs and SFs with the bin size of 15 days as well as ZDCFs are plotted in Figures 3–5, respectively. The detailed results are also listed in Table 2. The possible periods are very consistent and they vary a little between 1090 days and 1260 days. The mean period and the standard error are 1211 days and 38 days. From Figure 2 to Figure 5, it can be seen that the peaks in DCF and ZDCF and minima in SF are very broad. So, 1211 ± 38 days can be considered as a possible period in the optical variations, although the periods determined by different methods in different colors show a little difference.

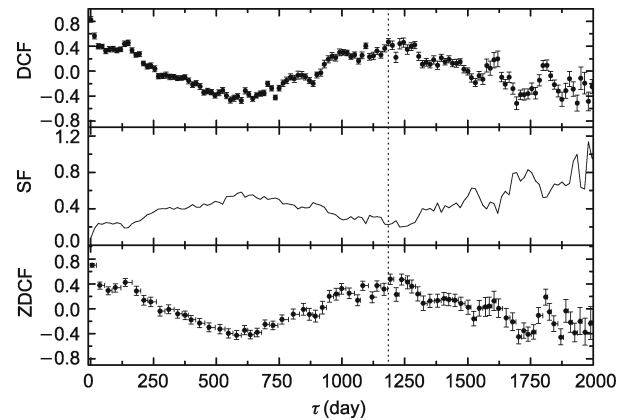
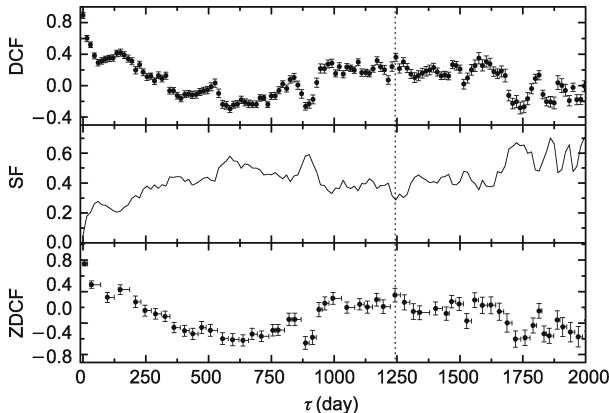
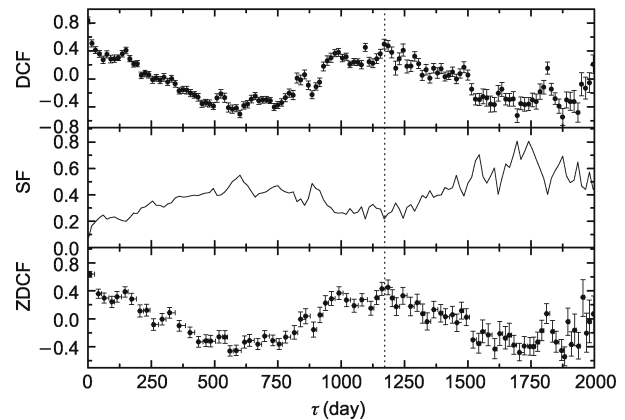


Figure 3 The DCF (top), SF (middle) and ZDCF (bottom) for the V passband. The vertical dotted line indicates the possible period according to the peak of DCF.

Table 2 Results determined by means of DCF, SF and ZDCF methods

Band	$\Delta\tau$ (day)	Period (day)	Period (day)	DCF	Period (day)	SF	Period (day)	Period (day)	ZDCF
<i>B</i>	10	1190	1194.5	0.49 ± 0.08	1230	0.21			
<i>B</i>	15	1200	1185.4	0.44 ± 0.07	1230	0.22	$1241^{+18.3}_{-4.9}$	1205.8	$0.41^{+0.10}_{-0.10}$
<i>B</i>	20	1180	1210.5	0.41 ± 0.06	1240	0.22			
<i>V</i>	10	1200	1210.6	0.50 ± 0.08	1240	0.19			
<i>V</i>	15	1185	1237.4	0.47 ± 0.06	1230	0.20	$1192^{+13.7}_{-3.0}$	1227.1	$0.48^{+0.08}_{-0.08}$
<i>V</i>	20	1240	1229.5	0.45 ± 0.07	1240	0.20			
<i>R</i>	10	1240	1244.7	0.40 ± 0.07	1250	0.28			
<i>R</i>	15	1245	1259.0	0.36 ± 0.05	1245	0.29	$1242^{+21.3}_{-3.9}$	1222.4	$0.36^{+0.08}_{-0.09}$
<i>R</i>	20	1240	1249.2	0.32 ± 0.05	1260	0.31			
<i>I</i>	10	1170	1175.2	0.52 ± 0.08	1090	0.21			
<i>I</i>	15	1170	1177.3	0.50 ± 0.07	1095	0.22	$1185^{+9.2}_{-3.7}$	1180.5	$0.45^{+0.10}_{-0.11}$
<i>I</i>	20	1180	1188.4	0.51 ± 0.06	1240	0.24			

**Figure 4** The DCF (top), SF (middle) and ZDCF (bottom) for the *R* passband. The vertical dotted line indicates the possible period according to the peak of DCF.**Figure 5** The DCF (top), SF (middle) and ZDCF (bottom) for the *I* passband. The vertical dotted line indicates the possible period according to the peak of DCF.

5 Discussion and conclusions

The variation of the source S5 0716+714 is very complex. When the three period analysis methods are applied to the light curves, the results show good consistency. They all suggest there is a possible period of ~ 1211 days in the optical light curve. The period of 1211 days is also very consistent with that of 3.3 years found by Raiteri et al. [26] in the optical *R*-band light curve.

From Table 2, one can see that the peak values of DCF and ZDCF are near or below 0.5. This means that 1211 days may be a weak period. The full light curves cover about 4462 days, and they have huge gaps after JD 2452000 (see Figure 1). Compared to the period of 1211 days, the light curves are not long enough, so that further monitoring is needed to check whether the source varies periodically.

The long term periodical variations may be explained by a binary black hole model or cyclic behavior of the accretion disk [2,46]. Several possible explanations for the periodic variations are also discussed by some authors [44]. They conclude that the periodic variations most likely arise from the intersections of a shock propagating down a relativistic jet that possesses a helical structure.

In conclusion, the historical optical *BVRI*-band light curves of S5 0716+714 are presented. This source varies violently and complicatedly. On the whole, it has brightened slightly during the past 10 years. The results show evidence of a 1211-day periodic variation in the light curves. To confirm whether or not there is a period variation in the light curve, further monitorings of this source are needed.

We express our thanks to the people helping with this work, and acknowledge the valuable suggestions from the peer reviewers. This work was supported by the Scientific Research Foundation of Fuyang Normal College, the National Natural Science Foundation of China (Grant No. 10975145), and partially by Natural Science Foundation of Yunnan Province (Grant No. 2007A026M).

- 1 Lainela M, Takalo L O, Sillanpää A, et al. The 65 day period in 3C 66A during bright state. *Astrophys J*, 1999, 521: 561–564
- 2 Sillanpää A, Haarala S, Korhonen T. Optical monitoring of quasars and BL Lac objects. *Astron Astrophys Suppl Ser*, 1988, 72: 347–354
- 3 Webb J R, Smith A G, Leacock R J, et al. Optical observations of 22 violently variable extragalactic sources - 1968–1986. *Astron J*, 1988, 95: 374–397
- 4 Kidger M R. The optical variability of 3C 345. *Astron Astrophys*, 1989,

- 226: 9–22
- 5 Kidger M, Takalo L, Sillanpää A. A new analysis of the 11-year period in OJ287—Confirmation of its existence. *Astron Astrophys*, 1992, 264: 32–36
- 6 Fan J H, Xie G Z, Pecontal E, et al. Historic light curve and long-term optical variation of BL Lacertae 2200+420. *Astrophys J*, 1998, 507: 173–178
- 7 Zhang X, Xie G Z, Bai J M. A historical light curve of 3C 345 and its periodic analysis. *Astron Astrophys*, 1998, 330: 469–473
- 8 Fan J H. Infrared variability properties of the blazar 3C 279. *Mon Not Roy Astron Soc*, 1999, 308: 1032–1036
- 9 Dai B Z, Zhang B K, Xiang Y, et al. The long-term optical variability properties of gamma-ray blazar 3C 273. *Int J Mod Phys D*, 2006, 15: 261–272
- 10 Kühr H, Pauliny-Toth I I K, Witzel A, et al. The 5-GHz strong source surveys. V - Survey of the area between declinations 70 and 90 deg. *Astron J*, 1981, 86: 854–863
- 11 Biermann P, Duerbeck H, Eckart A, et al. Observations of six flat spectrum sources from the 5 GHz survey. *Astrophys J Lett*, 1981, 247: L53–L56
- 12 Nilsson K, Pursimo T, Sillanpää A, et al. Detection of the host galaxy of S5 0716+714. *Astron Astrophys*, 2008, 487: L29–L32
- 13 Ghisellini G, Villata M, Raiteri C M, et al. Optical-IUE observations of the gamma-ray loud BL Lacertae object S5 0716+714: Data and interpretation. *Astron Astrophys*, 1997, 327: 61–71
- 14 Heidt J, Wagner S J. Statistics of optical intraday variability in a complete sample of radio-selected BL Lacertae objects. *Astron Astrophys*, 1996, 305: 42–52
- 15 Nesci R, Maesano M, Massaro E, et al. Intraday variability of BL Lacertae in the great 1997 outburst. *Astron Astrophys*, 1998, 332: L1–L4
- 16 Giommi P, Massaro E, Chiappetti L, et al. Synchrotron and inverse Compton variability in the BL Lacertae object S5 0716+714. *Astron Astrophys*, 1999, 351: 59–64
- 17 Villata M, Mattox J R, Massaro E, et al. The 0716+714 WEBT campaign of February 1999. *Astron Astrophys*, 2000, 363: 108–116
- 18 Wagner S J, Witzel A, Heidt J, et al. Rapid variability in s5 0716+714 across the electromagnetic spectrum. *Astron J*, 1996, 111: 2187–2211
- 19 Stalin C S, Gopal-Krishna, Sagar R, et al. Multiband optical monitoring of the blazars S5 0716+714 and BL Lacertae. *Mon Not Roy Astron Soc*, 2006, 366: 1337–1345
- 20 Wu J, Zhou X, Ma J, et al. Optical monitoring of BL Lacertae object S5 0716+714 with a novel multipeak interference filter. *Astron J*, 2007, 133: 1599–1608
- 21 Quirrenbach A, Witzel A, Wagner S, et al. Correlated radio and optical variability in the BL Lacertae object 0716 + 714. *Astrophys J Lett*, 1991, 372: L71–L74
- 22 Sagar R, Gopal-Krishna, Mohan V, et al. Multi-colour optical monitoring of the intra-day variable blazar S5 0716+71. *Astron Astrophys Suppl Ser*, 1999, 134: 453–461
- 23 Katajainen S, Takalo L O, Sillanpää A, et al. Tuorla quasar monitoring: I. Observations of 1995–1997. *Astron Astrophys Suppl Ser*, 2000, 143: 357–368
- 24 Qian B, Tao J, Fan J. Optical monitoring of S5 0716+714 from 1994 to 2000. *Astron J*, 2002, 123: 678–689
- 25 Ma L, Xie G Z, Zhou S B, et al. A new analysis of the medium-timescale periodicity in s5 0716+714. *Int J Mod Phys D*, 2004, 13: 659–668
- 26 Raiteri C M, Villata M, Tosti G, et al. Optical and radio behaviour of the BL Lacertae object 0716+714. *Astron Astrophys*, 2003, 402: 151–169
- 27 Montagni F, Maselli A, Massaro E, et al. The intra-night optical variability of the bright BL Lacertae object S5 0716+714. *Astron Astrophys*, 2006, 451: 435–442
- 28 Takalo L O, Sillanpää A, Nilsson K. Simultaneous UBVRI photopolarimetry of three blazars: 3C 66A, S5 0716+714 and OJ 287. *Astron Astrophys Suppl Ser*, 1994, 107: 497–501
- 29 Edelson R, Turner T J, Pounds K, et al. X-ray spectral variability and rapid variability of the soft X-ray spectrum Seyfert 1 galaxies Arakelian 564 and Ton S180. *Astrophys J*, 2002, 568: 610–626
- 30 Soldi S, Türler M, Paltani S, et al. The multiwavelength variability of 3C 273. *Astron Astrophys*, 2008, 486: 411–425
- 31 Nesci R, Massaro E, Rossi C, et al. The long-term optical variability of the BL Lacertae object S5 0716+714: Evidence for a processing jet. *Astron J*, 2005, 130: 1466–1471
- 32 Edelson R A, Krolik J H. The discrete correlation function - A new method for analyzing unevenly sampled variability data. *Astrophys J*, 1988, 333: 646–659
- 33 Hufnagel B R, Bregman J N. Optical and radio variability in blazars. *Astrophys J*, 1992, 386: 473–484
- 34 Peterson B M, Wanders I, Horne K, et al. On uncertainties in cross-correlation lags and the reality of wavelength-dependent continuum lags in active galactic nuclei. *Publ Astron Soc Pac*, 1998, 110: 660–670
- 35 Alexander T. Is AGN variability correlated with other AGN properties? ZDCF analysis of small samples of sparse light curves. *Astronomical Time Series*. Maoz D, Sternberg A, Leibowitz E M, eds. Dordrecht: Kluwer, 1997. 163
- 36 Liu H T, Bai J M, Zhao X H, et al. Tests for standard accretion disk models by variability in active galactic nuclei. *Astrophys J*, 2008, 677: 884–894
- 37 Roy M, Papadakis I E, Ramos-Colón E, et al. The recent high state of the BL Lacertae object AO 0235 and cross-correlations between optical and radio bands. *Astrophys J*, 2000, 545: 758–771
- 38 Hughes P A, Aller H D, Aller M F. The University of Michigan radio astronomy data base. I — Structure function analysis and the relation between BL Lacertae objects and quasi-stellar objects. *Astrophys J*, 1992, 396: 469–486
- 39 Simonetti J H, Cordes J M, Heeschen D S. Flicker of extragalactic radio sources at two frequencies. *Astrophys J*, 1985, 296: 46–59
- 40 Kataoka J, Takahashi T, Wagner S J, et al. Characteristic X-ray variability of TeV blazars: Probing the link between the jet and the central engine. *Astrophys J*, 2001, 560: 659–674
- 41 Cagnoni I, Papadakis I E, Fruscione A. Four years of extreme ultraviolet observations of Markarian 421. II. Temporal analysis. *Astrophys J*, 2001, 546: 886–897
- 42 Kataoka J, Tanihata C, Kawai N, et al. RXTE observations of 3C 273 between 1996 and 2000: Variability time-scale and jet power. *Mon Not Roy Astron Soc*, 2002, 336: 932–944
- 43 Smith A G, Nair A D, Leacock R J, et al. The longer optical time scales of a large sample of quasars. *Astron J*, 1993, 105: 437–455
- 44 Rani B, Wiita P J, Gupta A C. Nearly periodic fluctuations in the long-term X-ray light curves of the blazars AO 0235+164 and 1ES 2321+419. *Astrophys J*, 2009, 696: 2170–2178
- 45 Ciprini S, Tosti G, Raiteri C M, et al. Optical variability of the BL Lacertae object GC 0109+224. Multiband behaviour and time scales from a 7-years monitoring campaign. *Astron Astrophys*, 2003, 400: 487–498
- 46 Sillanpää A, Takalo L O, Pursimo T, et al. Confirmation of the 12-year optical outburst cycle in blazar OJ 287. *Astron Astrophys*, 1996, 305: L17–L20